

## Effects of Processing Steps and Organoclay Content in Butadiene Rubber/Organoclay Nanocomposites

Min-Su Kim, Gue-Hyun Kim

Division of Energy and Bio Engineering, Dongseo University, Busan, South Korea

Correspondence to: G.-H. Kim (E-mail: guehyun@gdsu.dongseo.ac.kr)

**ABSTRACT:** Even though polybutadiene rubber (BR) is a hydrophobic polymer, BR/organoclay nanocomposites are prepared successfully without a compatibilizer by using conventional compounding method. The main objective of this article is to investigate the effect of processing steps on the dispersion of organoclays in the BR matrix. The effect of each processing step on the dispersion of organoclays is studied by using X-ray diffraction (XRD). Also, the effect of the organoclay content on the mechanical properties is studied. According to the XRD results, mixing BR/organoclay compounds with vulcanization accelerator (MBTS) in a two-roll mill leads to the exfoliation of organoclays in this article. However, when BR/organoclay nanocomposites were heated at 155°C for the vulcanization as a next processing step, organoclays aggregated to become intercalated structure. The tensile and tear strength of BR/organoclay (9 phr) nanocomposite are 16.6 times and 3 times larger than those of BR, respectively. Over 100% and 300% modulus of BR, 300% and 350 % improvements are observed for those of BR/organoclay (9 phr) nanocomposite, respectively. © 2013 Wiley Periodicals, Inc. *J. Appl. Polym. Sci.* 129: 3512–3517, 2013

**KEYWORDS:** clay; composites; crosslinking; rubber

Received 27 August 2012; accepted 30 January 2013; published online 28 February 2013

DOI: 10.1002/app.39106

### INTRODUCTION

In recent years, polymer/organophilic-layered silicate (organoclay) nanocomposites have attracted considerable attention from both an academic and application point of view because of their improvement in material properties. Owing to the nanometer thickness and extremely high aspect ratio of silicate layers, the nanocomposites exhibit improvements in their mechanical, thermal, and barrier properties.<sup>1–4</sup>

Rubbers have been reinforced by various fillers to improve their mechanical properties and among several fillers, carbon black is the most important filler in this regard. It is seen that in order to produce the same mechanical strength as polymer/3–5% organoclay nanocomposites, 20–40% fillers have to be incorporated for conventional composites. Therefore, rubber/organoclay nanocomposites can make lighter rubber parts with improved elastic properties compared with conventional composites. Because of these advantages, many studies have been done for rubber/organoclay nanocomposites.<sup>5–25</sup> It has been reported that for the rubber/organoclay nanocomposites, processing conditions such as processing step significantly affect the dispersion state of organoclay in the rubber matrix.<sup>14–18</sup> It was also found

that the microstructures of some rubber/organoclay nanocomposites were influenced by the curing reactions.<sup>19–21</sup>

Polybutadiene rubber (BR) accounts for approximately 25% of the world's production of synthetic rubber. About 70% of the total production is used in tire compounds with another 20% being used for modifying plastics. It is very difficult to prepare polymer/organoclay nanocomposites by using hydrophobic polymers such as polyethylene and polypropylene without a compatibilizer. However, in our previous work,<sup>13</sup> BR (a hydrophobic polymer) nanocomposites were prepared successfully without a compatibilizer by using conventional compounding method. The mechanical properties such as tensile strength and rebound resilience were significantly improved by the addition of 3 phr organoclay.<sup>13</sup>

However, the effect of processing steps on the dispersion of organoclays and the effect of organoclay content on their mechanical properties were not studied in our previous study. In this article, the effect of each processing step on the dispersion of organoclays was studied by using X-ray diffraction (XRD). The effect of the organoclay content on the mechanical properties was also studied.

Additional Supporting Information may be found in the online version of this article.

© 2013 Wiley Periodicals, Inc.

**Table I.** Important Characteristics of the Materials used in this Study

|                       | Materials  | Supplier                  | Characteristics  |
|-----------------------|--|---------------------------|--|
| Rubber                | Butadiene rubber   | Kumho Petrochem., Korea   | cis-1,4 content: 95%, ML1 + 4(100°C): 45, Specific gravity: 0.91         |
| Organoclay            | Cloisite 15A   | Southern Clay, USA        | Specific gravity: 1.66   |
| Reinforced filler     | Carbon black N330  | Korea Carbon Black, Korea | Iodine adsorption : 82mg/g<br>Nitrogen surface area: 79m <sup>2</sup> /g |
| Cross-linking agent   | Sulfur   | Saekwang Chem., Korea     | Common grade   |
| Cross-linking coagent | Zinc oxide   | Gil-Chun Chem., Korea     |  |
|                       | Stearic acid   | LG Chem., Korea           | Specific gravity: 0.84, mp: 70°C   |
| Accelerator           | Dibenzothiazyl disulfide (MBTS)  | Dong Yang Chem., Korea    | Mol. Wt.: 332, mp: 160°C   |
| Antioxidant           | Pentaerythrityl-tetrakis[3-(3,5-di- <i>t</i> -butyl-4-hydroxy phenyl)-propionate] (Songnox 1010) | Songwon, Korea            | Mol. Wt.: 1178, mp: 110-125°C  |

## EXPERIMENTAL

### Materials and Preparation of BR/Organoclay Nanocomposites

Important characteristics of the materials used in this article are summarized in Table I. Organoclay was purchased from Southern Clay Products (USA) under the trade name of Cloisite 15A. Organic modifier of Cloisite 15A is dimethyl, dihydrogenated tallow, quaternary ammonium. The modifier concentration is 125 mequiv./100 g clay for Cloisite 15A.

BR, organoclay, zinc oxide (ZnO), antioxidant, and stearic acid were mixed in a Haake internal mixer at 120°C for 15 min. BR was first introduced and followed by the addition of organoclay and other additives. After being mixed in an internal mixer, the BR/organoclay mixtures were compounded for 2 min in a two-roll mill at 60°C before dibenzothiazyl disulfide (MBTS) was added, and mixing was continued for another 3 min. Finally, sulfur was mixed in a two-roll mill at 60°C for 5 min. BR/carbon black (60 phr) composites were prepared using the same method. The recipes of the compounds are described in Table II. After a two-roll mill process, the nanocomposites were vulcanized at 155°C in an electrically heated hydraulic press (14.7 MPa). If there is no specification of vulcanization time, their optimal cure time,  $t_{90}$  was used as the vulcanization time.

**Table II.** Recipes (in phr) of the Rubber Compounds

| Sample Materials          | BR  | BR/ organoclay | BR/ carbon black |
|---------------------------|-----|----------------|------------------|
| Butadiene rubber          | 100 | 100            | 100              |
| Zinc oxide                | 5   | 5              | 5                |
| Stearic acid              | 1   | 1              | 1                |
| Sulfur                    | 1   | 1              | 1                |
| MBTS                      | 1   | 1              | 1                |
| Antioxidant               | 0.5 | 0.5            | 0.5              |
| Organoclay (Cloisite 15A) |     | 3, 6, 9        |                  |
| Carbon black              |     |                | 60               |

The  $t_{90}$  values were derived from the Oscillating Disk rheometer (Gotech) measurements.

### Characterization of the Nanocomposites

XRD patterns were taken with a Rigaku D/max 2200H X-ray diffractometer (40 kV, 50 mA). The scanning rate was 0.5°/min. The basal spacing of the organoclay layer,  $d$ , was calculated using Bragg's equation,  $n\lambda = 2d\sin\theta$ . Transmission electron microscopy (TEM) images were taken from cryogenically microtomed ultrathin sections using EF-TEM (EM 912 Omega, Carl Zeiss, Germany). Cure characteristics were studied with the Oscillating Disk rheometer (Gotech) according to ASTM D2084. The rheometer rotor oscillates through a 1° arc at 1.66 Hz and exerts a shear strain on the sample during the curing of the sample.

### Measurement of Mechanical Properties

A Universal Testing Machine (Model UL25, Hounsfield) was used to obtain the tensile properties of the nanocomposites at room temperature. To prevent a possible strong orientation of organoclays because of fast strain rate during tensile tests, low cross-head speed (10 mm/min) was used in this article. All measurements were performed for five replicates of dog-bone shaped specimens and averaged to get the final result. Also the tear strength was measured using unnicked 90° angle test pieces at a cross-head speed of 500 mm/min in the Universal Testing Machine.

## RESULTS AND DISCUSSION

### Effect of Processing Steps on Dispersion of Organoclays for the Nanocomposites

Figure 1 shows the XRD patterns of each processing step of BR/organoclay (3 phr) nanocomposites. The peak at  $2\theta = 2.9^\circ$  corresponding to (001) plane (interlayer spacing  $d$ : 3.0 nm) is observed for pristine organoclay. After BR, organoclay, ZnO, and stearic acid were mixed in a Haake internal mixer at 120°C, the peak at  $2\theta = 2.9^\circ$  shifts to the lower angle at  $2\theta = 2.3^\circ$  ( $d$ : 3.8 nm). Also, the peak corresponding to (002) plane is

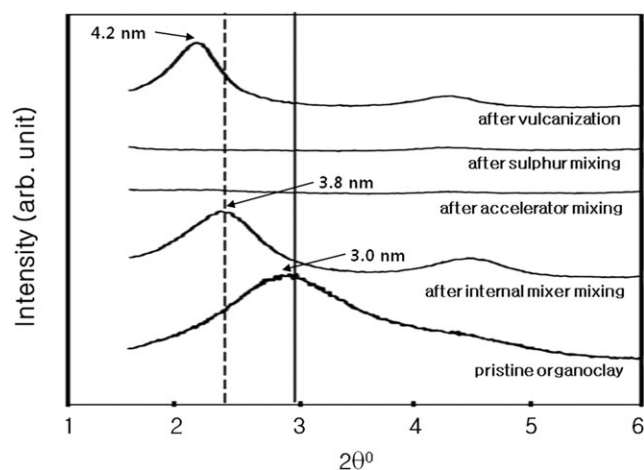


**Figure 1.** XRD patterns of each processing step of BR/organoclay (3 phr) nanocomposites.

observed. This result indicates the intercalation of BR molecules into the interlayer of organoclays, resulting in the expansion of the silicate interlayer.

After BR/organoclay compounds were mixed with vulcanization accelerator (MBTS) in a two-roll mill as a next processing step, the peak is disappeared in the XRD pattern. This indicates the exfoliation of organoclays. As the temperature at roll mill is 60°C, compared with 120°C at Haake internal mixer, the viscosity is higher during roll mill processing than during internal mixer processing. Because of the high viscosity during roll mill processing, high shear stress acts on the organoclay layers, resulting in the peel-off of the layers. It has been reported that the layered structure of organoclay can be broken up and peel-off on high acting shear forces.<sup>26,27</sup> After sulfur was added, the peak is not still observed in the XRD pattern.

However, after the nanocomposites were vulcanized at 155°C in an electrically heated hydraulic press for 15 min, the peak at  $2\theta = 2.1^\circ$  ( $d: 4.2$  nm) is observed. Therefore, organoclays, which were exfoliated in a two-roll mill process, aggregate to become intercalated structure during heating in a press for vulcanization. Also, there was a report that high vulcanization pressure causes aggregation of initially finely dispersed organoclays in rubber/organoclay nanocomposites.<sup>28</sup>

To confirm further the dispersion state of organoclays in the BR matrix, TEM study was carried out. Figure 2 presents the TEM photograph of an ultrathin section of the BR/organoclay (3 phr) nanocomposites after vulcanization. The dark lines are organoclay layers. Figure 2 exhibits intercalated organoclays as expected from XRD results. The interlayer distances of a few stacks of organoclays are accessed from the TEM photograph, which is local information. The interlayer distance of pristine organoclay is 3.0 nm. However, the interlayer distances assessed from the TEM photograph (Figure 2) are approximately 4.0–4.3 nm. The larger interlayer distance of organoclays than that of pristine organoclays observed in the TEM photograph is because of the intercalation of BR molecules into interlayers of organoclays. Also, exfoliated organoclays are observed and

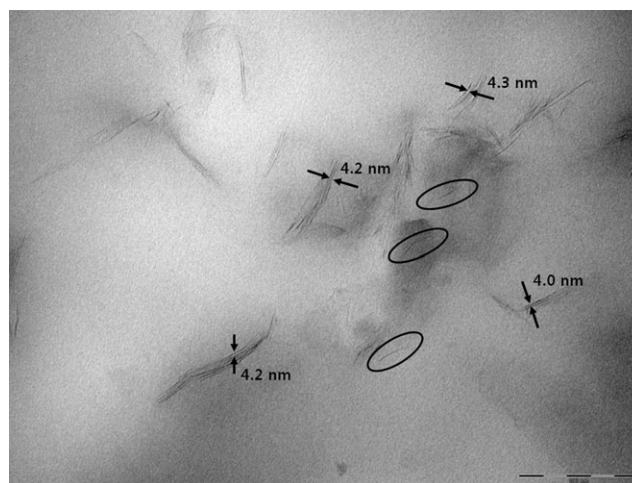


**Figure 2.** TEM photograph of an ultrathin section of the BR/organoclay (3 phr) nanocomposites.

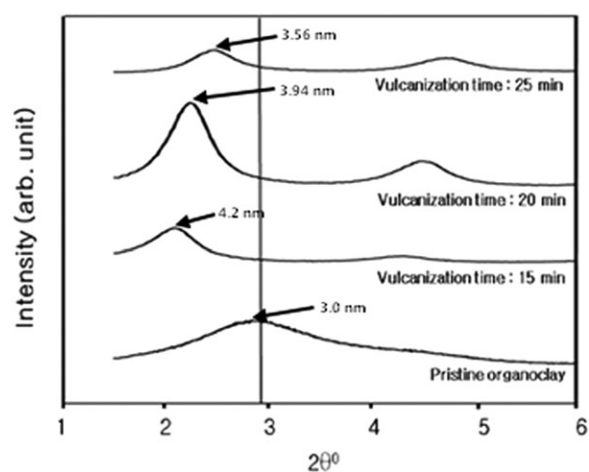


**Figure 3.** Effect of vulcanization time in a press on the XRD patterns of BR/organoclay (3 phr) nanocomposites.

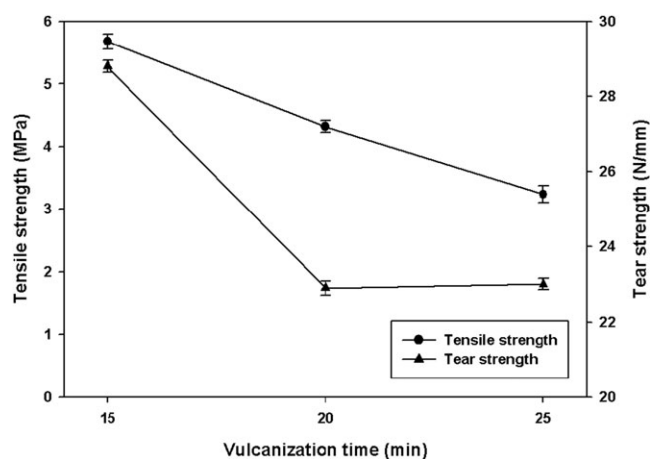


**Figure 4.** Tensile strength and tear strength of BR/organoclay (3 phr) nanocomposites as a function of vulcanization time in a press.

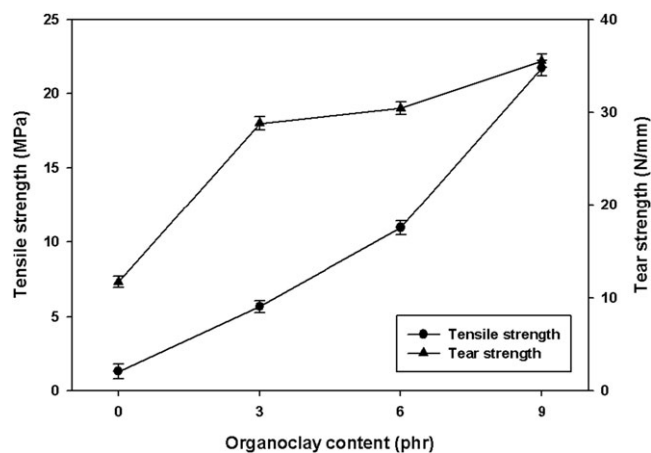


**Figure 5.** Tensile strength and tear strength of BR/organoclay nanocomposites as a function of organoclay content.

indicated by circles in the TEM photograph. However, the extent of exfoliation is significantly low and the nanocomposites consist predominantly of intercalated multiple platelet stacks.

As the peak is observed after heating for vulcanization for 15 min as shown in Figure 1, the effect of longer vulcanization time on the XRD patterns was investigated. Figure 3 shows the effect of vulcanization time in a press on the XRD patterns of BR/organoclay (3 phr) nanocomposites. With the increasing vulcanization time, the peak shifts to the higher angle, indicating smaller interlayer distance of organoclays.

The XRD results observed in Figure 1s and 3 can be explained as follows. In a two-roll mill process, strong shear helps the peel-off of the layers, resulting in exfoliation of organoclay. But this may not be a thermodynamically stable state. Exfoliated organoclays may be kinetically trapped in the viscous BR. During heating in a press for vulcanization, most rubber chains are still in the linear state and have mobility in the initial period of vulcanization. Therefore, as a process of reaching thermodynamically stable state, organoclays aggregate to become intercalated structure, resulting in the reappearance of peaks as observed in Figure 1. However, as the vulcanization progresses, the viscosity of the BR nanocomposites increases and reaching thermodynamically stable state is delayed by the high viscosity of BR. Therefore, as shown in Figure 3, interlayer distance slowly decreases with vulcanization time as a process to reach thermodynamically stable state. Similar reaggregation of filler particles has been reported for polymer/conductive filler composites.<sup>29–32</sup> Figure 4 shows the tensile strength and tear strength of BR/organoclay (3 phr) nanocomposites as a function

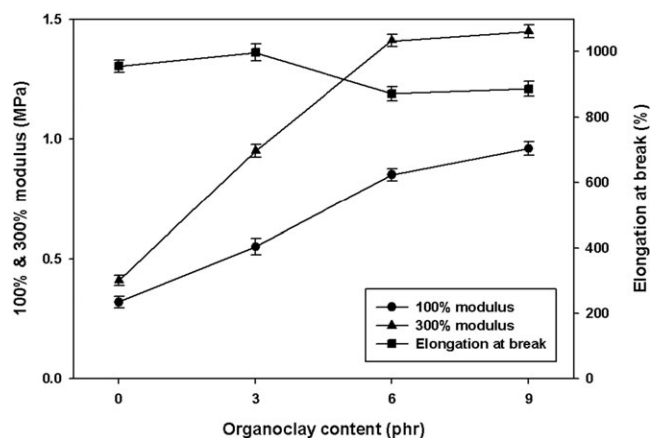


**Figure 6.** 100%, 300% modulus and elongation at break of BR/organoclay nanocomposites as a function of organoclay content.

of vulcanization time in a press. With the increasing vulcanization time, the tensile and tear strengths decrease. There are two possible explanations for the reduction of mechanical properties with the increasing vulcanization time. The reduction may correspond to a reversion effect. However, a reversion was not observed in the Oscillating Disk rheometer curve at 155°C for 25 min. The other possible explanation for the reduction of mechanical properties is the decrease of interlayer distance of organoclays as shown in Figure 3. According to the constitutive model for tensile behavior of polymer/organoclay nanocomposites,<sup>33</sup> the increase of the organoclay layer spacing produces the same effect by increasing the volume fraction of organoclays. Also, it has been reported that increased interlayer distance of organoclay leads to the improved mechanical properties.<sup>22,23</sup>

### Effect of Organoclay Content on Mechanical Properties for the Nanocomposites

A remarkable increase of the mechanical properties is observed for the BR/organoclay nanocomposites. Figure 5 shows the tensile strength and tear strength of BR/organoclay nanocomposites as a function of organoclay content. With the increasing organoclay content, the tensile and tear strengths continuously increase. The tensile strength of EPDM/organoclay nanocomposites was reported to increase with increasing organoclay content up to 5 phr, but decrease with further increase of organoclay content.<sup>15</sup> However, in this article, the tensile strength of BR/organoclay nanocomposites increases up to 9 phr. The tensile and tear strengths of BR/organoclay (9 phr) nanocomposite are 16.6 times and 3 times greater than those of BR, respectively.

**Table III.** Mechanical Properties of BR/Organoclay Nanocomposite and BR/Carbon Black Composites

| Sample                   | Tensile strength (MPa) | 100% Modulus (MPa) | 300% Modulus (MPa) | Elongation at break (%) | Tear strength (N/mm) |
|--------------------------|------------------------|--------------------|--------------------|-------------------------|----------------------|
| BR/organoclay (9 phr)    | 21.7 (±0.5)            | 0.96 (±0.03)       | 1.45 (±0.03)       | 886 (±23)               | 35.5 (±0.7)          |
| BR/carbon black (60 phr) | 9.1 (±0.3)             | 0.71 (±0.02)       | 1.83 (±0.04)       | 773 (±20)               | 38.1 (±0.5)          |

**Table IV.** Cross-Linking Characteristics of BR/Organoclay Nanocomposites

| Sample                | MH (N-m) | ML (N-m) | Torque difference (N-m) |
|-----------------------|----------|----------|-------------------------|
| BR                    | 0.720    | 0.199    | 0.521                   |
| BR/organoclay (3 phr) | 0.955    | 0.278    | 0.677                   |
| BR/organoclay (6 phr) | 0.981    | 0.280    | 0.701                   |
| BR/organoclay (9 phr) | 0.992    | 0.285    | 0.707                   |

Figure 6 shows the 100%, 300% modulus and elongation at break of BR/organoclay nanocomposites as a function of organoclay content. Over 100% and 300% modulus of BR, 300% and 350% improvements are observed for those of BR/organoclay (9 phr) nanocomposite, respectively. Generally in composites, their modulus is related to the dispersion of fillers and interaction between fillers and matrix. Well-dispersed fillers and high interaction between fillers and matrix give higher enhancement of modulus to the composites. Also, high aspect ratio of organoclays contributes to the significant improvement of modulus for BR/organoclay nanocomposites. With the increasing organoclay content, elongation at break slightly decreases. This is because of the decrease in ductility with increased stiffness.

As carbon black is the most important filler for rubber, the mechanical properties of BR/organoclay (9 phr) nanocomposites were compared with those of BR/carbon black (60 phr) composites as shown in Table III. BR/organoclay (9 phr) nanocomposites display better mechanical properties than BR/carbon black (60 phr) composites except 300% modulus and tear strength.

The curing behaviors of BR/organoclay nanocomposites were studied at 155°C with the Oscillating Disk rheometer and the characteristics are summarized in Table IV. The nanocomposites show higher maximum torque and higher torque difference between the maximum and minimum torque than BR. This suggests that the organoclay significantly increases the crosslink density of BR, because the torque difference is related to the crosslink density.<sup>24,25</sup> Organoclays behave as an effective agent for BR vulcanization. Such an effect has been already reported for some other rubber nanocomposites.<sup>12,19</sup> This effect was attributed to the ammonium groups in the organoclay.<sup>12,19</sup> Therefore, increased crosslink density also contributes to the significant improvement of mechanical properties of BR/organoclay nanocomposites.

## CONCLUSIONS

BR/organoclay nanocomposites were prepared successfully by using conventional compounding method without a compatibilizer. According to the XRD results for each processing step, mixing BR/organoclay compounds with vulcanization accelerator (MBTS) in a two-roll mill leads to the exfoliation of organoclays in this article. However, when BR/organoclay nanocomposites were heated at 155°C for the vulcanization, organoclays aggregated to become intercalated structure. As exfoliated structure as a result of strong shear may not be a thermody-

namically stable state, during heating in a press for vulcanization, organoclays aggregate to become intercalated structure.

Because of intercalation of organoclays and increased crosslink density, significant improvement of mechanical properties was realized. The tensile and tear strengths of BR/organoclay (9phr) nanocomposite are 16.6 times and 3 times greater than those of BR, respectively. Over 100% and 300% modulus of BR, 300% and 350 % improvements are observed for those of BR/organoclay (9 phr) nanocomposite, respectively.

## ACKNOWLEDGMENT

This work was funded by Dongseo University.

## REFERENCES

- Alexandre, M.; Dubois, P. *Mater. Sci. Eng. R Rep.* **2000**, *28*, 1.
- LeBaron, P. C.; Wang, Z.; Pinnavaia, T. J. *Appl. Clay. Sci.* **1999**, *15*, 11.
- Giannelis, E. P. *Adv. Mater.* **1996**, *8*, 29.
- Ray, S. S.; Okamoto, M. *Prog. Polym. Sci.* **2003**, *28*, 1539.
- Joly, S.; Garnaud, G.; Ollitrault, R.; Bokobza, L.; Mark, J. E. *Chem. Mater.* **2002**, *14*, 4202.
- Arroyo, M.; López-Manchado, M. A.; Herrero, B. *Polymer* **2003**, *44*, 2447.
- Zhang, L.; Wang, Y.; Sui, Y.; Yu, D. *J. Appl. Polym. Sci.* **2000**, *78*, 1873.
- Ganter, M.; Gronski, W.; Reichert, P.; Mulhaupt, R. *Rubber Chem. Technol.* **2001**, *74*, 221.
- Kim, J. T.; Oh, T. S.; Lee, D. H. *Polym. Int.* **2003**, *52*, 1058.
- Kim, J. T.; Lee, D. Y.; Oh, T. S.; Lee, D. H. *J. Appl. Polym. Sci.* **2003**, *89*, 2633.
- Vu, Y. T.; Mark, J. E.; Pham, L. H.; Engelhardt, M. *J. Appl. Polym. Sci.* **2001**, *82*, 1391.
- Varghese, S.; Karger-Kocsis, J.; Gatos, K. G. *Polymer* **2003**, *44*, 3977.
- Kim, M. S.; Kim, D. W.; Chowdhury, S. R.; Kim, G. H. *J. Appl. Polym. Sci.* **2006**, *102*, 2062.
- Usuki, A.; Tugigase, A.; Kato, M. *Polymer* **2002**, *43*, 2185.
- Ahmadi, S. J.; Huang, Y.; Li, W. *Compos. Sci. Technol.* **2005**, *65*, 1069.
- Schön, F.; Thomann, R.; Gronski, W. *Macromol. Symp.* **2002**, *189*, 105.
- Gatos, K. G.; Thomann, R.; Karger-Kocsis, J. *Polym. Int.* **2004**, *53*, 1191.
- Gatos, K. G.; Karger-Kocsis, J. *Polymer* **2005**, *46*, 3069.
- Varghese, S.; Karger-Kocsis, J. *J. Appl. Polym. Sci.* **2004**, *91*, 813.
- Gatos, K. G.; Sawanis, N. S.; Apostolov, A. A.; Thomann, R.; Karger-Kocsis, J. *Macromol. Mater. Eng.* **2004**, *289*, 1079.
- LeBaron, P. C.; Pinnavaia, T. J. *Chem. Mater.* **2001**, *13*, 3760.

22. Vasilakos, S. P.; Tarantili, P. A. *J. Appl. Polym. Sci.* **2012**, *125*, E548.
23. Li, P.; Song, G.; Yin, L.; Sun, C.; Wang, L. *Iran. Polym. J.* **2007**, *16*, 775.
24. Ismail, H.; Freakley, P. K.; Sutherland, I.; Sheng, E. *Eur. Polym. J.* **1995**, *31*, 1109.
25. Mousa, A.; Karger-Kocsis, J. *Macromol. Mater. Eng.* **2001**, *286*, 260.
26. Fornes, T. D.; Yoon, P. J.; Keskkula, H.; Paul, D. R. *Polymer* **2001**, *42*, 9929.
27. Fornes, T. D.; Yoon, P. J.; Hunter, D. L.; Keskkula, H.; Paul, D. R. *Polymer* **2002**, *43*, 5915.
28. Liang, Y. -R.; Lu, Y. -L.; Wu, Y. -P.; Ma, Y.; Zhang, L. -Q. *Macromol. Rapid Commun.* **2005**, *26*, 926.
29. Asai, S.; Sumita, M. *J. Macromol. Sci. Phys.* **1995**, *B34*, 283.
30. Zhang, C.; Ma, C. A.; Wang, P.; Sumita, M. *Carbon* **2005**, *43*, 2544.
31. Pötschke, P.; Fornes, T. D.; Paul, D. R. *Polymer* **2002**, *43*, 3247.
32. Pötschke, P.; Dudkin, S.M.; Alig, I. *Polymer* **2003**, *44*, 5023.
33. Jo, C.; Fu, J.; Naguib, H. E. *Polym. Eng. Sci.* **2006**, *46*, 1787.